



Journal of
**Fisheries and
Aquatic Science**

ISSN 1816-4927



Academic
Journals Inc.

www.academicjournals.com

Bed Scouring and Fish Habitats at Dam-less River Water Intake

Habibi Lila and Keshavarzi AliReza
Water Department, Shiraz University,
Shiraz, I.R. Iran

Abstract: In this study, an experimental approach was used to understand separation zone and bed scouring at water intake. To find the effect of intake angle and discharge ratio on the separation size and bed scouring, five different types of water intakes with different angles were installed at one side of a main canal. The velocity of the flow inside the intake was measured in 727 points in a fine grid, including 243 points at three horizontal layers and 486 points in 6 cross sections using electromagnetic velocity meter. At different discharge ratios, the length and width of the separation zone were compared under five intake angles. The scouring at the bed was also measured using sandy surface meter. It was found that the size and location of separation is very much dependent on the discharge ratio and intake angle. Also it was found that the minimum scouring occurred at water intake with 56 degree angle under discharge ratio 0.2. Finally some relationships were found for the with, length and depth of bed scouring at water intakes.

Key words: Dam-less water intake, separation zone, optimum angle, streamline

Introduction

The water intake is usually used to divert water from main canal and river into the lateral canals and turbine intake. The streamlines of the flow at a straight open channel are approximately parallel to the flow direction. When an intake is installed at one side of the canal, the streamlines of the flow deflect toward the intake. At this flow condition, two groups of secondary currents are produced at the region close to the water intake. The first group of secondary currents rotates in horizontal surface; however the second group rotates in vertical direction. In this study, the first group of secondary currents is referred to plain secondary currents. Therefore, the plain secondary current in this study is defined the circulation of flow in a horizontal surface and parallel to the water surface.

The structure of flow in open-channel junction was studied by Taylor (1944), Law and Reynolds (1966), Hager (1984), Hsu *et al.* (2002) and Weber *et al.* (2001). Taylor (1944) considered the flow depth at the upstream and downstream of a canal junction as a parameter of flow condition and produced a theoretical development. The vertical secondary current at water intake with 90 degree diversion was investigated by Neary and Odgaard (1993).

However, little study was carried out to understand flow structure and bed scouring at water intakes with angles different from 90 degrees. In this study, the flow structure and particularly the secondary currents and their effect on bed scouring at water intake with angles 45, 56, 67, 79 and 90 degrees were investigated experimentally.

From a dimensional analysis it was found that the size of the separation zone is a function of deflection angle (θ), Froude number in the main channel and lateral $\frac{1}{Fr^2}$, relative width $\frac{W_b}{W}$, relative roughness $\frac{n}{n_s}$ relative scour width and depth $\frac{L_{sh}}{W_{sh}}, \frac{H_{sh}}{Y_b}$ and relative discharge $\frac{Q_u}{Q_d}$.

$$\frac{L_s}{W_s} = f\left(\frac{W_b}{W}, \frac{L_{sh}}{W_{sh}}, \frac{H_{sh}}{Y_b}, \frac{1}{Fr^2}, \frac{Q_u}{Q_d}, \frac{n}{n_s}, \theta\right)$$

Where, L_s is the length, W_s is the width of the separation, W_b is the width of water intake, W is the width of main canal, L_{sh} , W_{sh} and H_{sh} are length, width and depth of the scouring respectively, Y_b is the water depth at water intake, n_s is the bed roughness, Q_u is the flow rate in the upstream in the main channel and Q_d is the flow rate in the lateral canal.

Materials and Methods

Experimental Setup

The experiments were carried out in a non-recirculating experimental flume with a lateral. Five water intakes with 45, 57, 67, 89 and 90 degrees were installed at one side of the main canal with the angles of 45, 57, 67, 89 and 90 degrees. The first water intake is installed at 6.40 m from the flume inlet. The main canal consisted of a rectangular cross section with base width of 0.50 m, height 0.40 m and 15.80 m length. The longitudinal slope of the flume was set to 0.0003. The lateral diversion canal consisted of 0.25 m width, 0.40 m height. The flow of the intake discharges downstream through a 7.63 m lateral canal. The flow rate at the end of main and lateral canals was measured using two pre-calibrated right-angle V-notches. The main canal and the lateral were built of smooth concrete. A schematic diagram of the experimental model is shown in Fig. 1.

In order to study scour depth in five water intakes, the bed of flume is covered with a layer of 10 cm sediment particles of D_{50} equal to 0.6 mm. The grain-size distribution curve of the sediment particles is shown in Fig. 2. The experimental tests were performed at flow rate

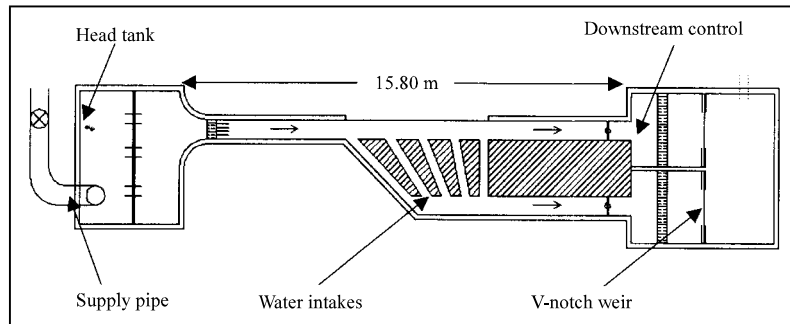


Fig. 1: A schematic of experimental setup

Table 1: Experimental flow conditions

Discharge ratio	Angle (Deg.)	Discharge (L sec ⁻¹)	Main channel discharge (L sec ⁻¹)	Intake channel discharge (L sec ⁻¹)	Flow depth upstream channel (cm)	Flow depth downstream main channel (cm)	Flow depth main channel (cm)	Up-stream main intake froude number	Down-stream main channel froude number	Intake channel froude number
0.8	45	16.2785	3.0045	13.274	15.95	15.90	15.20	0.030	0.030	0.286
	56	16.481	2.961	13.52	15.78	15.60	15.23	0.030	0.031	0.291
	67	16.482	2.965	13.517	15.69	15.52	15.19	0.030	0.031	0.292
	79	18.621	3.092	15.529	16.5	16.57	15.41	0.029	0.029	0.328
0.6	45	17.359	7.372	9.987	17.13	17.10	16.79	0.066	0.067	0.185
	56	18.015	7.298	10.717	16.80	16.90	16.68	0.068	0.067	0.201
	67	16.341	6.793	9.548	16.26	16.85	15.10	0.066	0.063	0.208
	79	15.581	6.377	9.204	16.70	16.90	16.60	0.060	0.059	0.174
0.4	45	9.211	6.377	2.834	16.25	16.70	16.68	0.062	0.060	0.053
	56	13.041	8.621	4.420	16.50	16.20	16	0.082	0.084	0.088
	67	17.894	11.380	6.514	18.02	17.35	17.33	0.095	0.101	0.115
	79	18.088	11.574	6.514	16.97	16.70	16.67	0.106	0.108	0.122
0.2	45	16.217	12.471	3.746	16.02	16.25	15.41	0.124	0.122	0.079
	56	16.572	12.471	4.101	16.59	17.11	15.54	0.118	0.113	0.086
	67	16.470	12.369	4.101	16.76	16.82	15.82	0.115	0.115	0.083
	79	16.418	12.369	4.049	16.58	16.62	16.31	0.117	0.117	0.079
90	16.217	12.471	3.746	16.02	16.16	15.87	0.124	0.123	0.076	

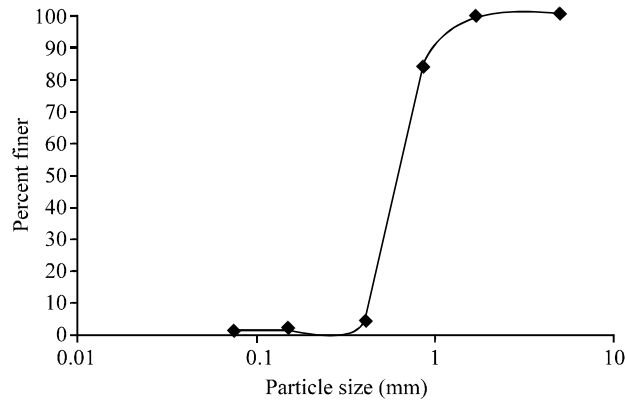


Fig. 2: Grain-size distribution of the sediment particles

equal to 16 L sec⁻¹. The ratio of flow between the main canal and water intakes is defined using the following equation:

$$Q_r = \frac{Q_L}{Q_M}$$

Where, Q_r is discharge ratio and Q_M and Q_L are flow discharge at main canal and water intakes, respectively. In this study, four different discharge ratios as: $Q_r = 0.2$, $Q_r = 0.4$, $Q_r = 0.6$ and $Q_r = 0.8$ were considered in the experiments. The depth of flow for all tests was kept constant to 16 cm using downstream control gate. The velocity of the flow in two components was measured using an

Table 2: Points of velocity measurement

Intake angle	45	56	67	79	90
Layer	158	148	143	138	133
Total	474	444	429	414	399

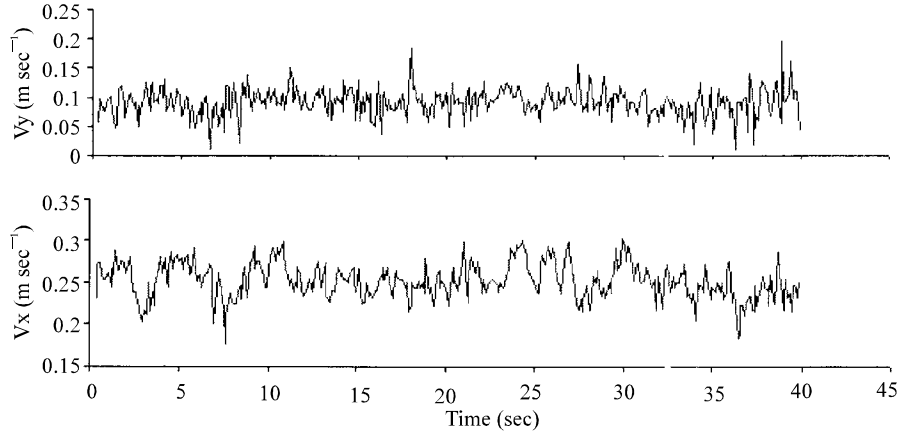


Fig. 3: Time series of velocity fluctuations

electromagnetic velocity meter (PE-30 Model, Ellipsoid type, DELFT). The velocity measurement was done at three layers in depth of flow at water intakes. The velocity of flow in two directions was measured in time for duration of 40 sec with sampling rate of 0.1 Hz. Therefore, a total number of 400 velocity data at each point of flow was recorded in the computer. The velocity in the horizontal layers was measured at a regular grid. The grid size for the velocity measurement in horizontal layers was 25 mm in width and 50 mm in the length of the intake. To find the size of separation zone in depth, the velocity of the flow was measured at three depths as: 3 cm from the bed, 6 cm from the bed and 12 cm from the bed. The experiments were performed at different flow conditions as shown in Table 1. The number of points for flow velocity measurement is also shown in Table 2. At similar points, the bed surface was measured using sandy surface meter. Figure 3 shows a time series of velocity for each point of flow at water intake.

Results and Discussion

Velocity Distribution at Different Angles of Water Intake

As mentioned previously, the velocity of flow at each point was measured with a sampling rate of 0.1 Hz and for a duration of 40 sec. Then from the measured time series of velocity fluctuation, the time-averaged velocity in the flow direction (\bar{U}) and in transverse direction (\bar{V}), at each point were calculated using the following equations:

$$\bar{U} = \frac{1}{n} \sum_{i=1}^n u_i$$

$$\bar{V} = \frac{1}{n} \sum_{i=1}^n v_i$$

Where, u_i and v_i are instantaneous velocities in the flow direction and transverse direction, respectively, and n is the number of sampling.

The value of velocity in flow direction (\bar{U}) is plotted for the different sections from the intersection of main canal and lateral to the end of the lateral canal. To cover the entire area at the mouth of lateral canal, at a section of -5 cm the velocity was measured in the main canal. The velocity distribution pattern is shown in Fig. 4 to 8 for five different angles of 45, 56, 67, 79 and 90 degrees, respectively and for different cross sections in the lateral canal under discharge ratio of 0.6. From the contour lines of velocity, the location of maximum velocity is appeared for each cross section. It was found that the location of maximum velocity is not at the same location for the all different cross sections. The location of maximum velocity is at the upstream at the inlet of lateral whereas it moves to the downstream at the end of the lateral. As a result, a region of separation zone is formed for each lateral canal.

Additionally, the value of velocity for 90 degree water intake is shown in Fig. 9 for the sections along the lateral canal and in the flow direction for the distance of 50, 100, 150 and 200 mm from upstream to the downstream. It was found that the maximum velocity occurred at the mouth of water intake with angles 79 and 90 degrees to the half of the width of the water intake. Also it was found that the velocity of flow decreases when the angle of water intake changes from 45 to 90 degree.

The Size of Separation Zone

The size of separation is derived from the velocity vector and particle trace method at the depths of 3, 6 and 12 cm from the bed for different discharge rates and for the five different angles. The most feature of the particle trace method is the observation of the separation zone along the water intake. The separation zones are very clear at the upstream or downstream portion of the water intake. The width and length of the separation zone were derived from the particle trace method. The particle trace method shows the location of the separation zone and deflected streamlines toward the intake. It can be seen that in the separation zone the streamlines are deflected from the wall at upstream of water intake. The size of the separation zone is small near the bed, while it is large near the surface. Due to the difference in velocity particularly where streamlines are very close, a momentum transfer occurs between the streamlines and produces a series of eddies. The eddies will move downstream of the intake and dissipate energy along the intake. The large separation size will cause higher momentum transfer between streamlines and therefore large eddies will form. At this condition a large amount of energy will dissipate along the intake and allows less flow rate discharges into the intake. To minimize the separation zone and scouring, design of intake with minimum scouring is necessary and it is the major focus of this study.

To find the water intake with minimum separation, the width and the length of the separation at upstream and downstream were measured under different discharge ratio and for the angles of 45, 56, 67, 89 and 90 degree and they are shown separately for upstream and downstream locations. The length of the separation is shown in Fig. 10 for upstream and downstream, while the width of the separation for upstream and downstream are shown in Fig. 11. The intersection of the best-fit equations represents the optimum angle of the water intake. From the Fig. 11, it was found that there is minimum separation zone at water intake with discharge ratio 0.2 is at the angles of 45 however, for larger discharge ratio the minimum separation zone is created at 56 degree water intake.

A statistical analysis of the data is shown that there some relations between the angle of water intake and the size of separation. In Table 3 some relationships are presented for the length and the width of the separation at different discharge ratios.

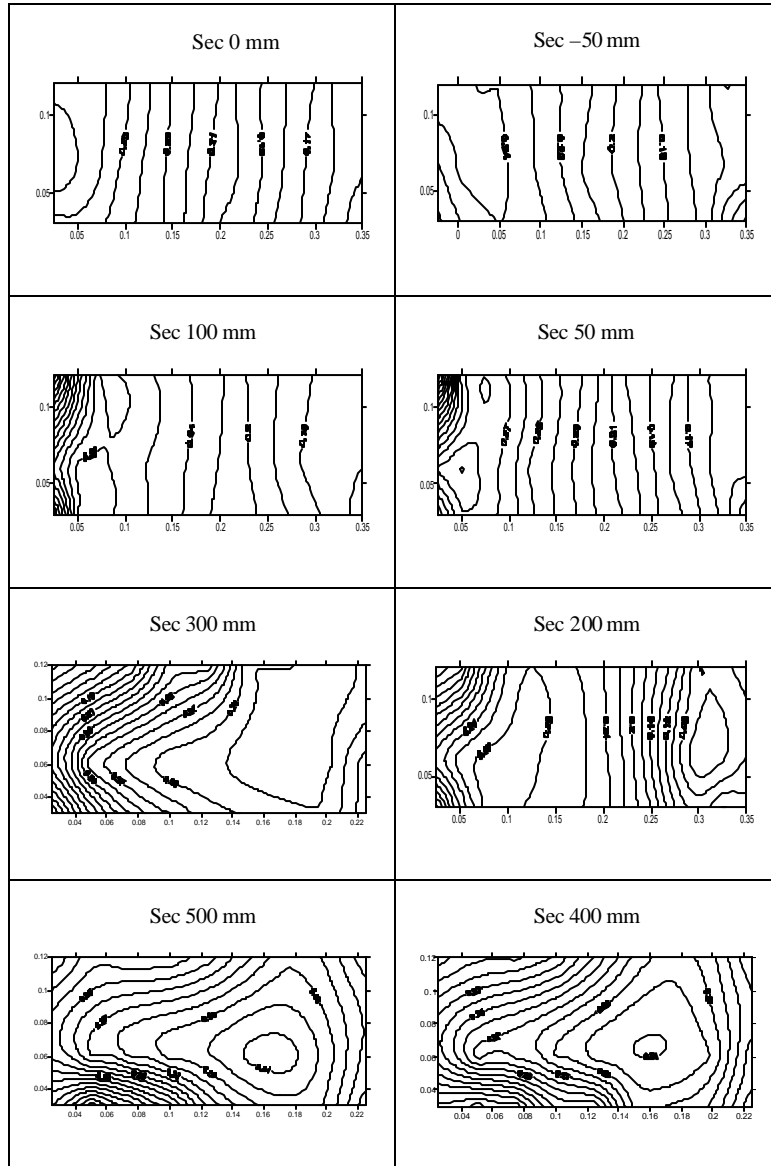


Fig. 4: The pattern of velocity at 45 angle water intake for discharge ratio 0.6

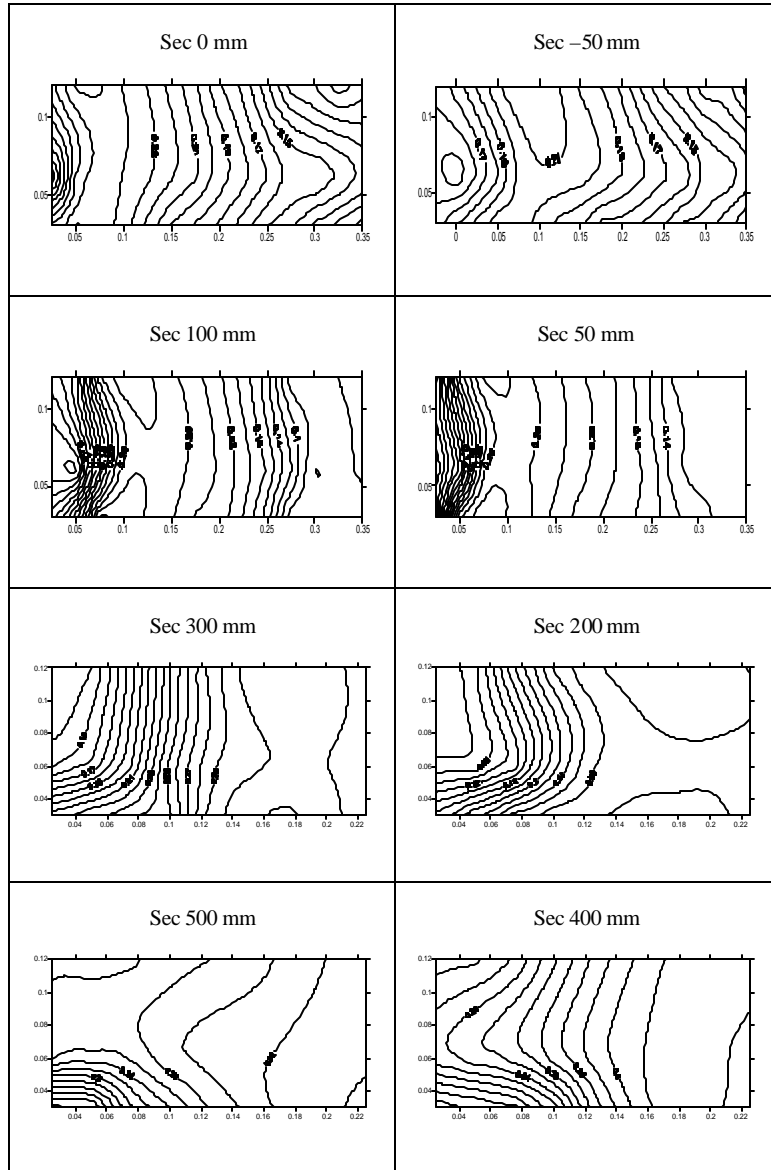


Fig. 5: The pattern of velocity at 56 angle water intake for discharge ratio 0.6

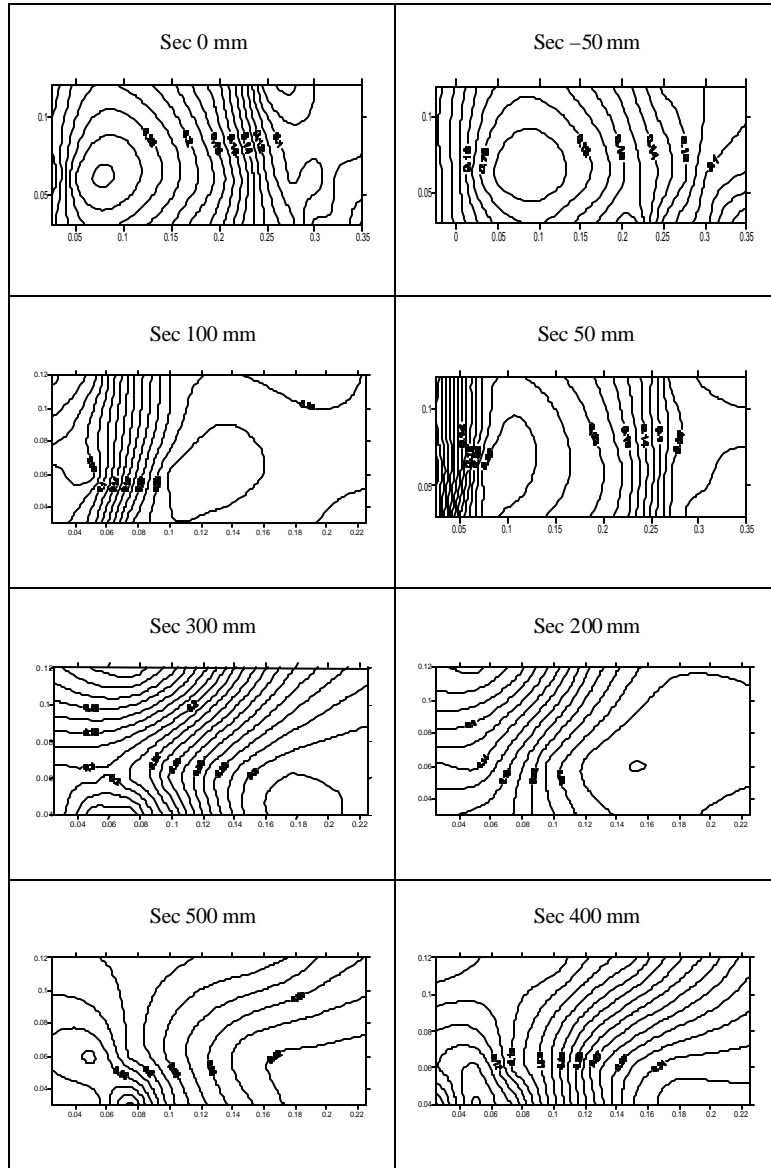


Fig. 6: The pattern of velocity at 67 angle water intake for discharge ratio 0.6

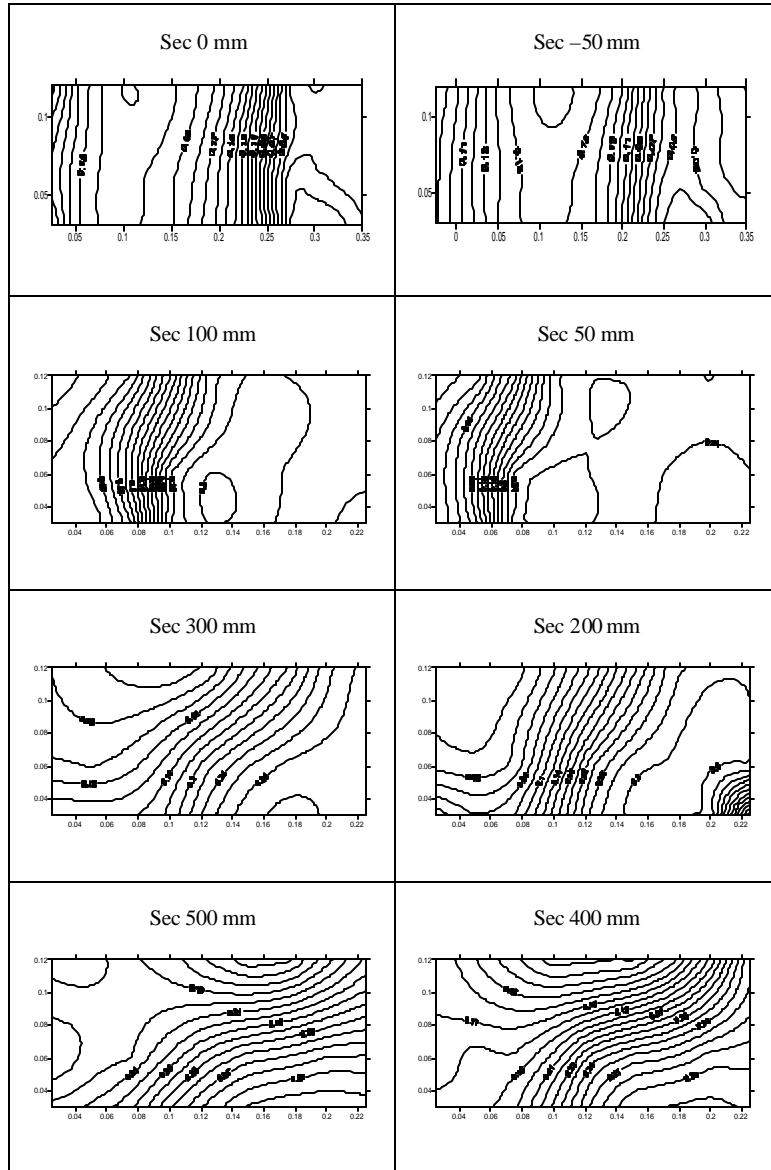


Fig. 7: The pattern of velocity at 79 angle water intake for discharge ratio 0.6

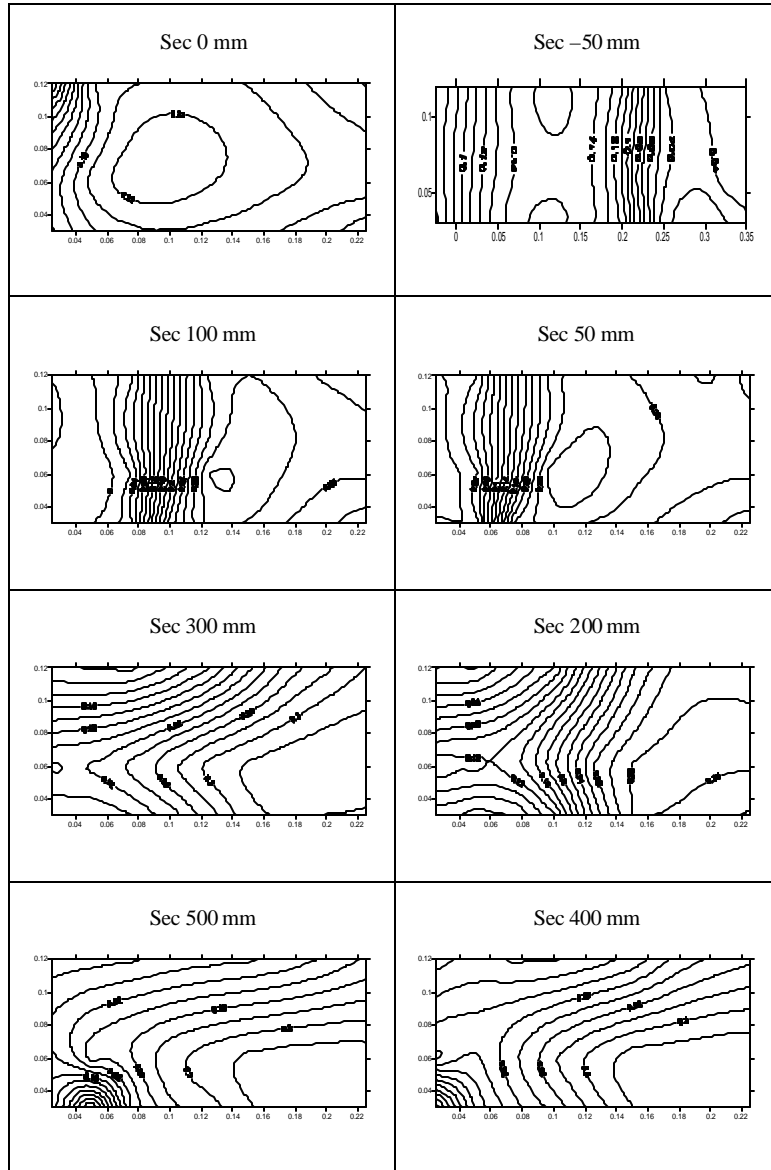


Fig. 8: The pattern of velocity at 90 angle water intake for discharge ratio 0.6

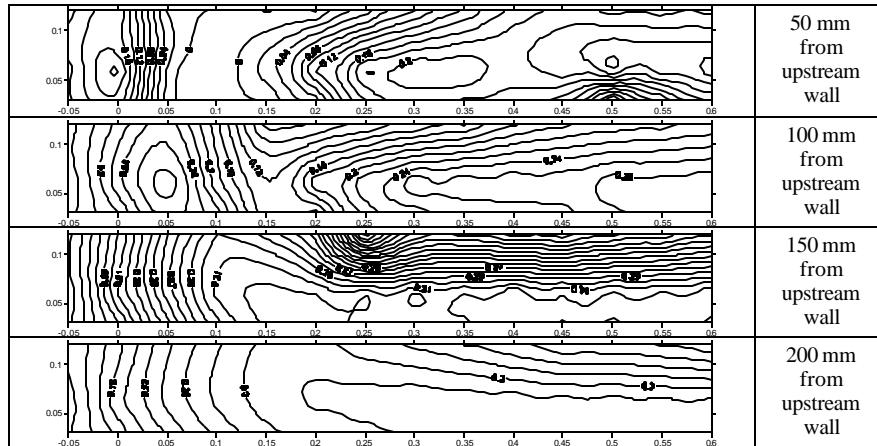


Fig. 9: The pattern of velocity at 90 degree water intake in the length of lateral channel

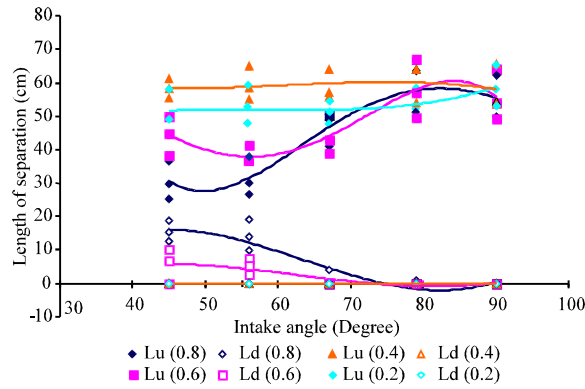


Fig. 10: Length of separation at upstream and downstream of water intake

Table 3: Relations of the length and width of separation with water intake angles at different discharge ratios.

Discharge ratio	Relation the length and the width of the separation	
0.2	W_u	$2E-05\theta^4-0.0057\theta^3+0.58\theta^2-25.55\theta+416.61$
	W_d	$8E-05\theta^3-0.0164\theta^2+1.0092\theta-17.451$
	L_u	$4E-05\theta^4-0.011\theta^3+1.2476\theta^2-59.473\theta+1041.4$
	L_d	$0.0007\theta^3-0.1295\theta^2+7.497\theta-121.14$
0.4	W_u	$3E-05\theta^4-0.0073\theta^3+0.74\theta^2-32.804\theta+534.93$
	W_d	$0.0001\theta^3-0.02\theta^2+1.33\theta-23.53$
	L_u	$-4E-05\theta^4+0.0086\theta^3-0.67\theta^2+21.16\theta-173.12$
	L_d	$0.0003\theta^3-0.047\theta^2+2.71\theta-43.02$
0.6	W_u	$-4E-07\theta^4+0.0002\theta^3-0.019\theta^2+1.055\theta-9.49$
	W_d	0
	L_u	$-0.0002\theta^3+0.0307\theta^2-1.77\theta+91.28$
	L_d	0
0.8	W_u	$0.0001\theta^3-0.026\theta^2+1.81\theta-31.46$
	W_d	0
	L_u	$0.0003\theta^3-0.045\theta^2+2.62\theta+1.47$
	L_d	0

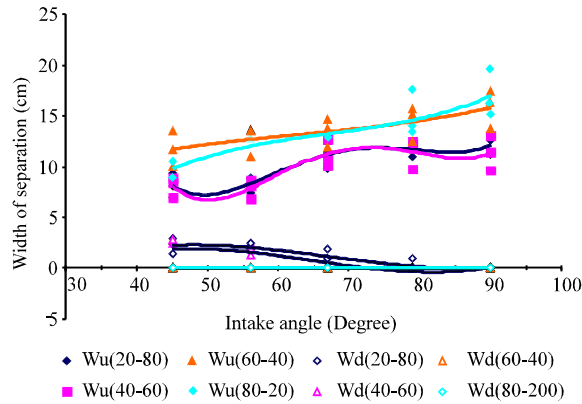


Fig. 11: Width of separation at upstream and downstream of water intake

where, θ is the angle of water intake and L_d and L_u are the length of separation at downstream and upstream of water intake and W_u and W_d are the width of the separation at the upstream and downstream of water intake, respectively.

Bed Scouring at Different Water Intake Angle

To determine the effect of water intake angle on the scouring, the bed scouring recorded at different discharge ratio. At the initial stage of the experiment, the bed was covered with 10 cm of sediment particles with D_{50} of 0.6 mm. The experiments were performed at water intake with angles 45, 56, 67, 79 and 90 degrees and different flow conditions. The experiment was carried out under discharge ratios of 0.2, 0.4, 0.6 and 0.8, which is the ratio of diverted flow at water intake to the main canal discharge. To determine the scouring process at water intake, after equilibrium time, the topography of the bed was measured using sandy surface meter. Figure 12 to 16 shows the bed profile and velocity of flow after achieving the equilibrium condition. The contour lines of the bed scouring are shown in Fig. 17 for different angles water intake. The three dimensional topography of the bed after the equilibrium condition is shown in Fig. 18. It was found that the scouring started in the main canal and at the inlet of water intake and then extended to the upstream and downstream of water intake. But the deposition started from the middle to the end of water intake. The above condition was achieved after the equilibrium condition.

For the water intake with 67, 79 and 90 degree the scouring increases along the water intake with the increasing of deflection angle. But in 45 degree water intake, the scouring occurred at the upstream of water intake. The minimum scouring was found to occur for the 56 degree water intake. Figure 19 shows the time evolution of the scour depth at different angle water intake.

To find the variation of scouring with different discharge ratio (Q_r), the experiments were performed in four discharge ratio (Fig. 20). It was also found that the scouring pattern varies with different discharge ratios. For Q_r larger than 0.5, it was found that the minimum scouring occurred at

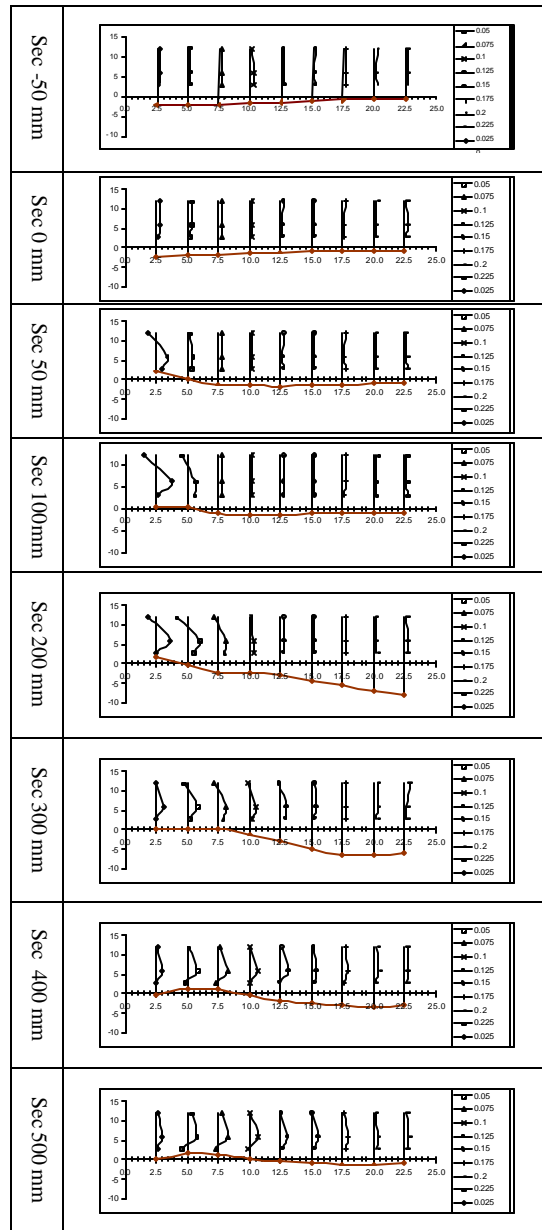


Fig. 12: Bed profile and velocity profile after the experiments for 45 degree water intake

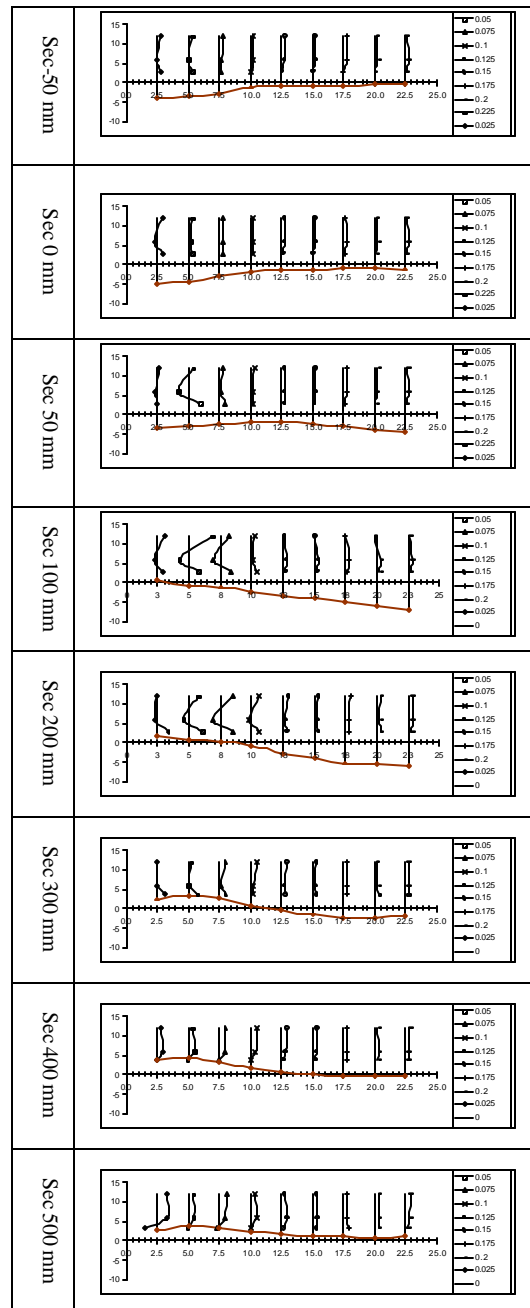


Fig. 13: Bed profile and velocity profile after the experiments for 56 degree water intake

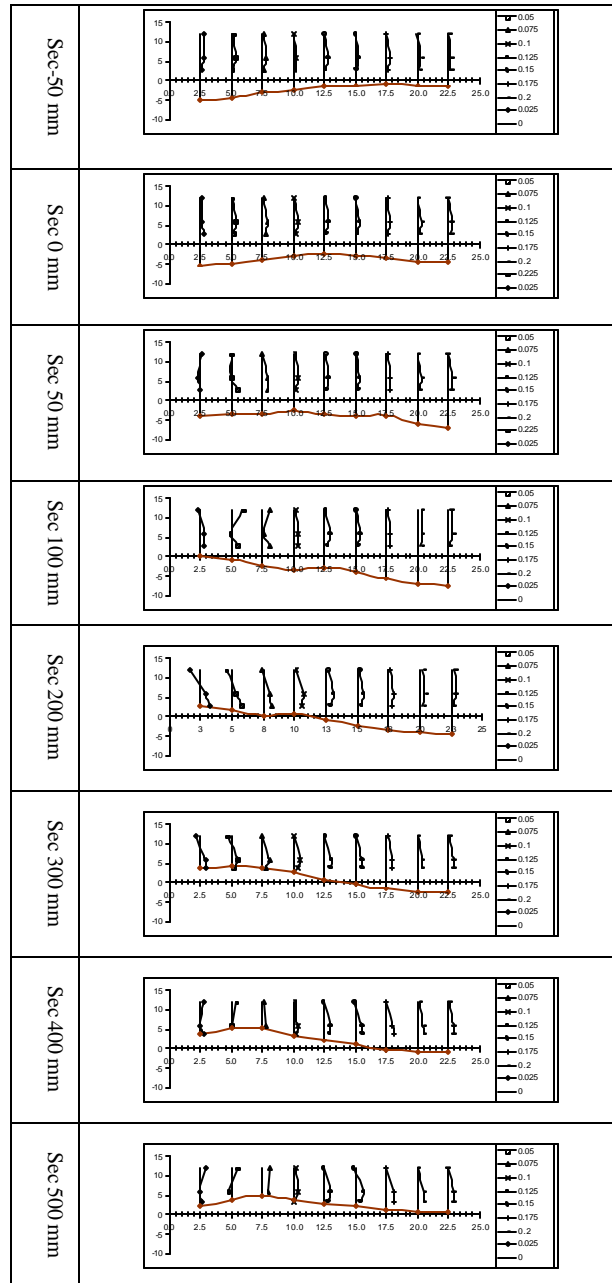


Fig. 14: Bed profile and velocity profile Bed profile after the experiments for 67 degree water intake

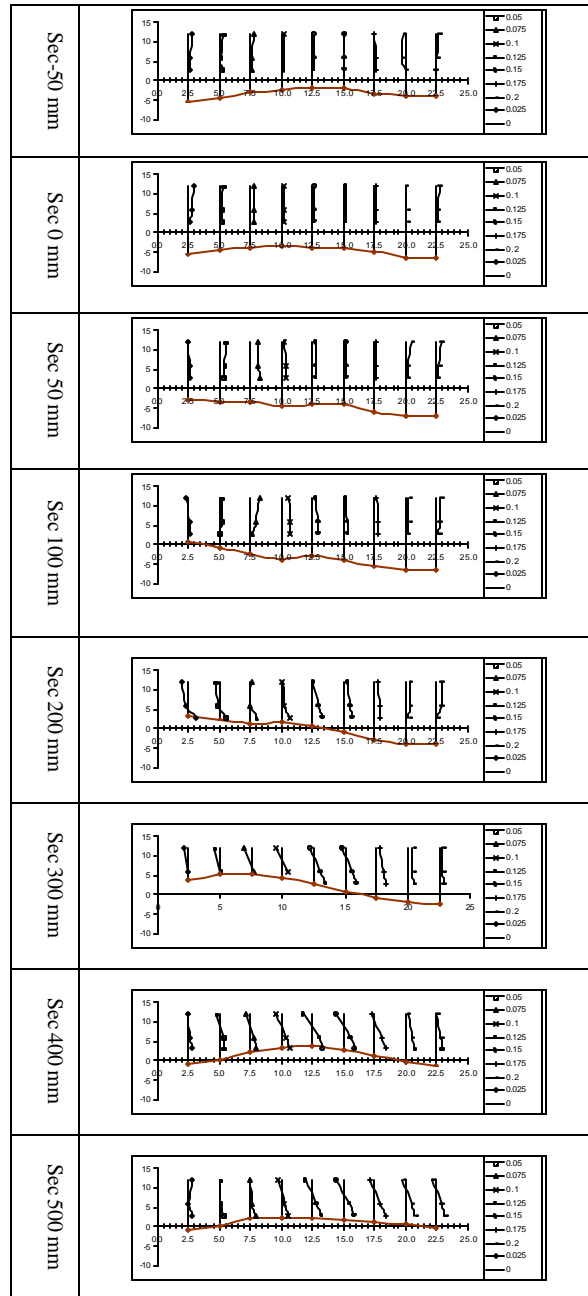


Fig. 15: Bed profile and velocity profile Bed profile after the experiments for 79 degree water intake

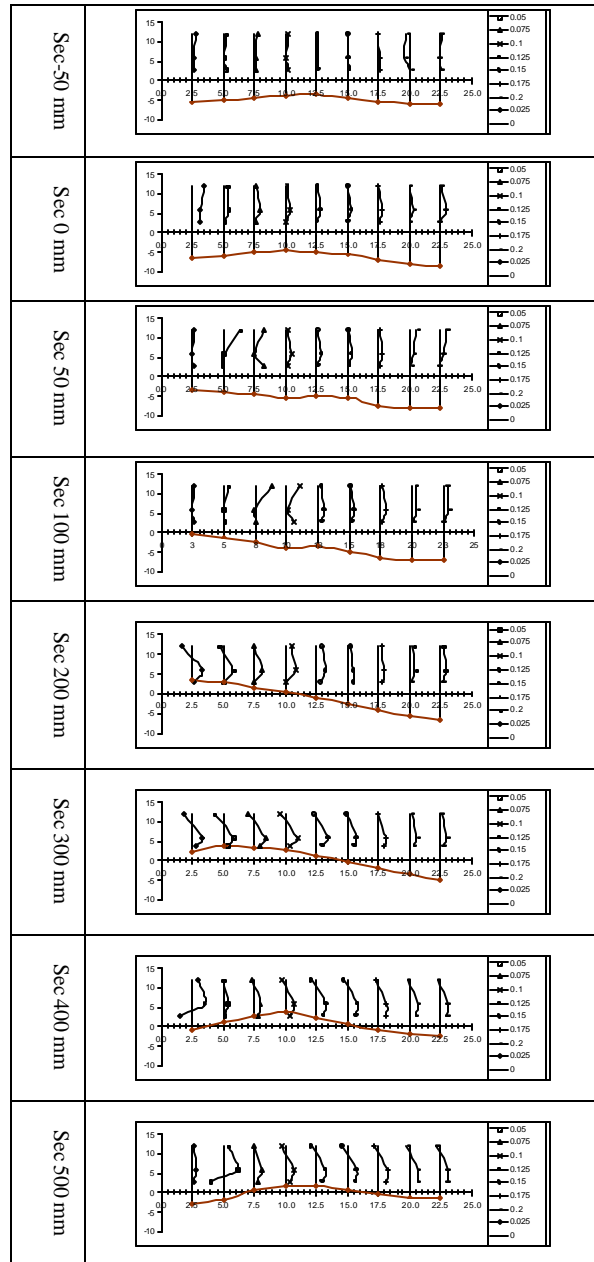


Fig. 16: Bed profile and velocity profile Bed profile after the experiments for 90 degree water intake

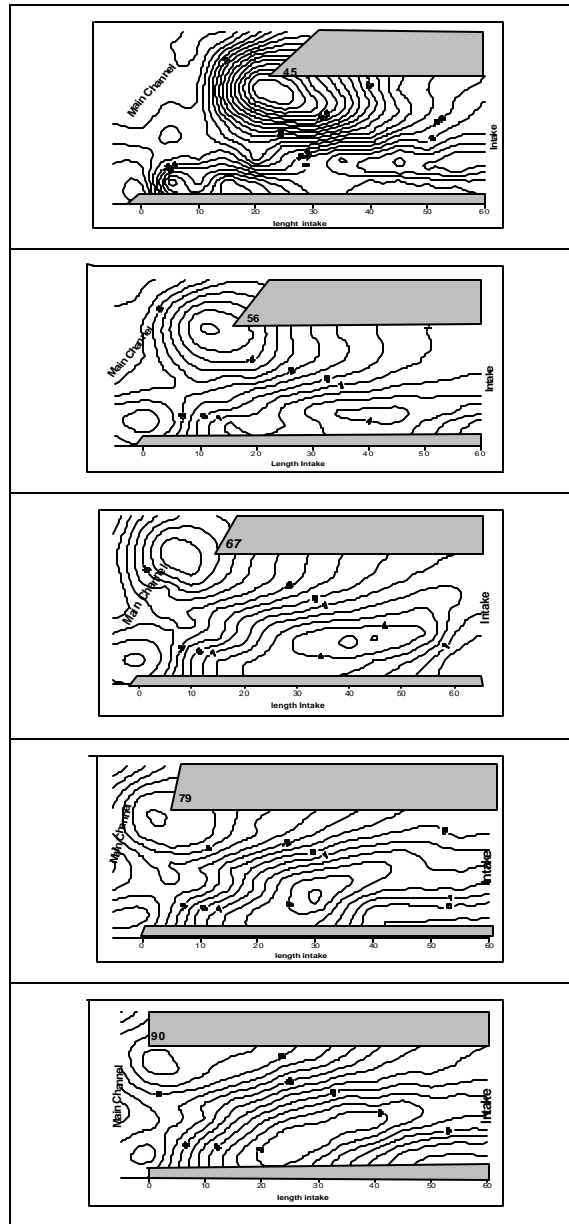


Fig. 17: Plan view of the final bed situation at different angle water intake

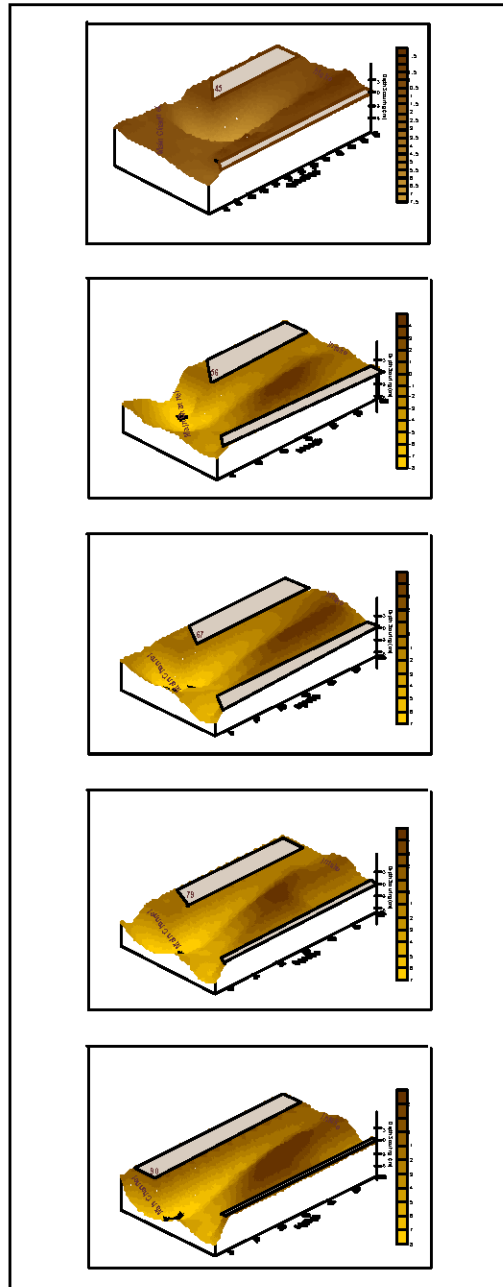


Fig. 18: Three dimensional topography of the bed after the equilibrium condition. The dashed line indicates the initial bed level at different angle water intake

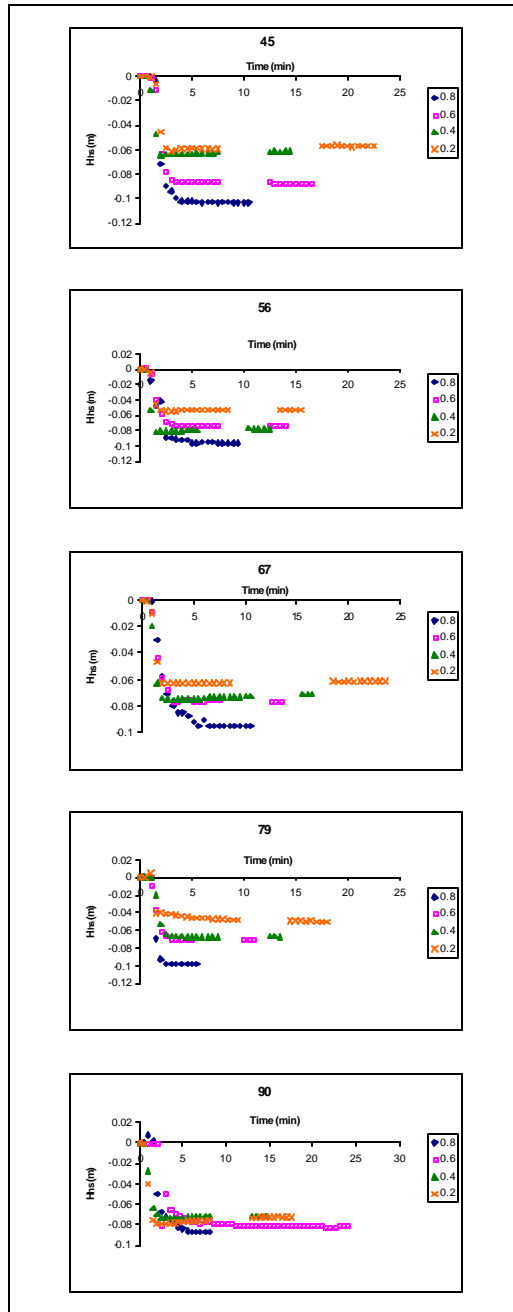


Fig. 19: Time evolution of scour depth at different angle water intake

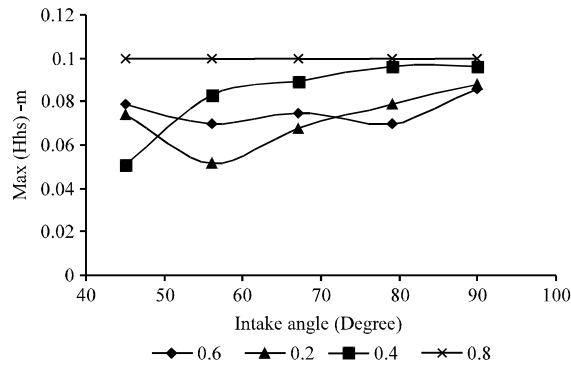


Fig. 20: Scour depth for different angle of water intake

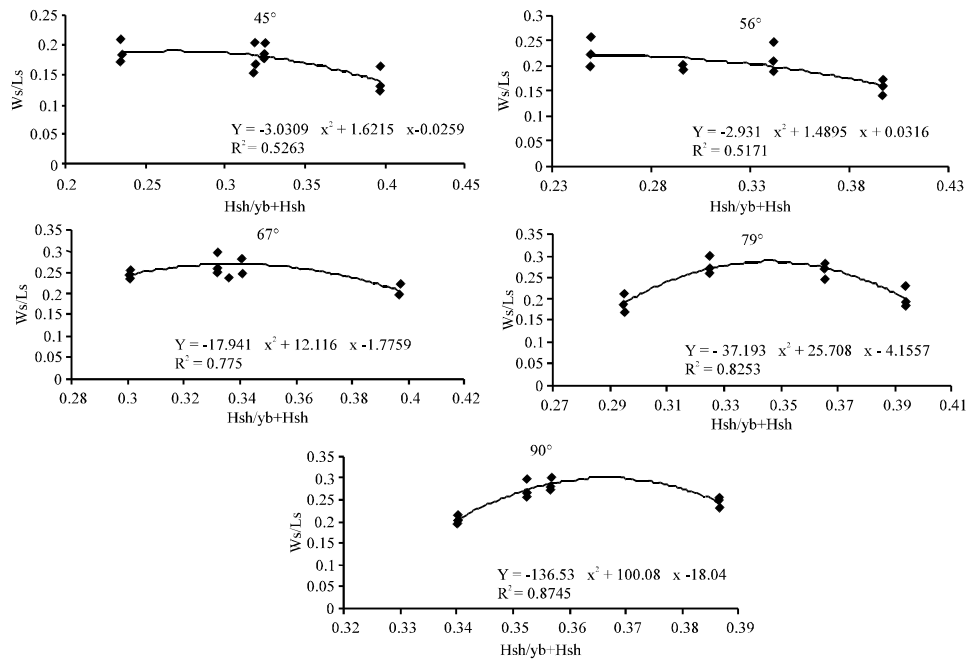


Fig. 21: Relationship of scour depth with separation size at different angle water intake

56 degree water intake but for the Qr smaller than 0.5, the minimum scouring occurred at 45 water intake. Figure 21 shows the relationships of scour depth with separation size at different angle water intake. Some relationships were also found for scouring depth with separation size.

Conclusions

In this study the length and width of the separation zone were compared under five deflection angles and at different discharge ratios. It was found that the size and location of separation is very

much dependent on the discharge ratio. The result showed that for high discharge ratio the separation occurs in the downstream side of water intake whereas in low discharge ratio, it occurs in the upstream. From the present results, it was found that there is minimum separation zone at water intake with discharge ratio 0.2 is at the angles of 45 however, for larger discharge ratio the minimum separation zone is created at 56 degree water intake. Also it was found that the minimum scouring occurred at water intake with 56 degree angle under discharge ratio 0.2 and maximum scouring and sedimentation occurred at all water intakes under discharge ratio of 0.8. Finally some relationships were found for the width, length and depth of bed scouring at water intakes.

References

- Hager, W.H., 1984. An approximate treatment of flow in branches and bends. Proc. Inst. Mech. Eng., 198C: 63-69.
- Hsu, Ch. Ch., C.J. Tang, W.J. Lee and M.Y. Shieh, 2002. Subcritical 90° equal-width open-channel dividing flow. J. Hydraulic Eng., ASCE., 128: 716-720.
- Law, S.W. and A.J. Reynolds, 1966. Dividing flow in an open channel. J. Hydraulic Division, ASCE., 92: 207-231.
- Neary, V.S. and A.J. Odgaard, 1993. Three dimensional flow structure at open channel diversions. J. Hydraulic Eng., ASCE., 119: 1223-1230.
- Taylor, E.H., 1944. Flow characteristics at rectangular open-channel junctions. Trans., ASCE., 109: 893-912.
- Weber, L.J., E.D. Schumate and N. Mawer, 2001. Experiment on flow at a 90° open-channel junction. J. Hydraulic Eng., ASCE., 127: 340-350.